3rd Specialty Conference on Material Engineering & Applied Mechanics
3e Conférence spécialisée sur le génie des matériaux et mécanique appliquée

Montréal, Québec
May 29 to June 1, 2013 / *29 mai au 1 juin 2013*

Influence of ECC Mixture on the Structural Performance of Link Slabs in Bridge Decks

Md. A. Kayes, Maulin B. Mavani, Khandaker M. A. Hossain and Mohamed Lachemi
Department of Civil Engineering, Ryerson University, Toronto, Ontario, Canada

ABSTRACT: The expansion joints are a major source of deterioration of multi-span bridges in Canada and North America. Expansion joints can be replaced by flexible link slabs forming a joint-free bridge. The high strain capacity while maintaining low crack widths makes engineered cementitious composite (ECC) an ideal material for the link slab construction. This paper presents the results of an experimental study on the structural performance of ECC link slabs compared to their conventional self-consolidating concrete (SCC) counterparts. Influence of ECC mixtures on the link slab performance was investigated based on load-deflection response, crack development, strain characteristics and failure modes. Experimental results showed that ECC link slab exhibited superior behaviour compared to their SCC counterparts in terms of strength, crack width, ductility and energy absorbing capacity.

1. Introduction

Every year, in USA and Canada, billions of dollars are spent to repair and maintenance bridges. Cost of repairs and maintenance increase with the increase of life time of bridges. The poor durability of concrete bridges throughout Canada is an increasingly large concern for highway transportation authorities. With decreasing budget allocations for infrastructure maintenance, rehabilitation, and replacement, the need for greater durability is superficial. High strength concrete has been used in maintenance and repair works of infrastructures such as bridge decks with different degrees of success (Li 2003; Li et al. 2002). But none of these solutions target the inherent shortfall of concrete brittleness, which results in cracking. These cracks, allow salt water to contact the reinforcing bars and causing corrosion and finally leading to structural failure.

A major source of bridge deterioration requiring constant maintenance is mechanical expansion joints installed between adjacent simple bridge decks (Wolde-Tinsae and Klinger 1987). A possible approach to alleviate this problem is the elimination of mechanical deck joints in multi-span bridges. Two solutions to eliminate deck joints are proposed (Alampalli and Yannotti 1998, Gilani 2001). First solution is an integral construction concept with girder continuity and second solution is a joint-less bridge deck concept using link slab with simply supported girders (Fig.1).

The section of the deck connecting the two adjacent simple-span girders is called the link slab (LS). Fig. 2 shows the components of a typical link slab. The length of the debond zone (throughout which all shear connectors are removed and a debonding mechanism is placed on the top flange of the girder) is 5.0% of each adjacent bridge span. It was found necessary to extend the length of the link slab 2.5% further into each adjacent span to help transfer load from the girders into the link slab through additional shear connectors. Within the extended zone, known as the transition zone, the number of shear connectors should be 50% more than the number required by AASHTO design procedures. Caner and Zia experimentally analyzed the performance of joint less bridge decks and proposed design methods for the conventional concrete link slab (Caner and Zia 1998, Lepech and Li, 2009).

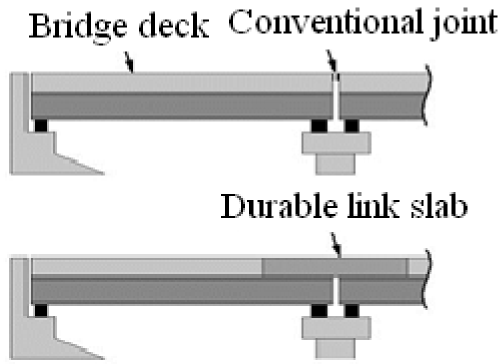

(a) Bridge deck with joint (b) Bridge deck with link slab

Figure 1: Joint less bridge deck with link slab

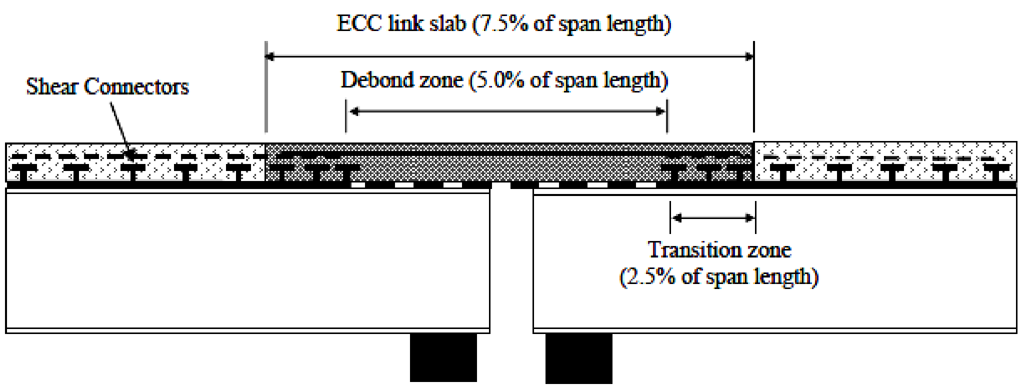

Figure 2: Schematic of ECC link slab showing components

Engineered cementitious composite (ECC) is a high performance fiber reinforced cementitious composites designed with micromechanical principals (Li and Kanda 1998). The high strain capacity while maintaining low crack widths of ECC make it an ideal material for the link slab application (Li 1993; Li 1998; Sahmaran et al. 2010; Fischer and Li 2003). Few research studies conducted to date showed significant enhancement of ductility and crack width control in ECC link slabs confirming that the use of ECC can be effective in extending the service life of bridge deck systems (Keoleian et al. 2005). Lack of research studies especially in Canada warrants extensive research investigations on structural performance of ECC based link slabs (Hossain et al. 2012). The full understanding of the behaviour of ECC link slabs is very important for this new technology to be adopted in bridge structures.

This paper presents the structural performance of ECC link slabs compared to their conventional self-consolidating concrete (SCC) counterparts based on load-deflection response, crack development, strain characteristics and failure modes.

2. Experimental Study

Comprehensive research consisting of experimental and theoretical investigations is in progress to study the structural performance of link slab with ECC of different types and varying geometric/material parameters under monotonic and fatigue loading conditions. Experimental results of link slabs made with one ECC mixture and a conventional SCC tested under monotonic loading condition are the subject matter of this paper.

2.1 Link Slab Configuration, Test Specimens, Material Properties and Casting

The deformed shape and moment distribution due to applied load of a two-span bridge structure with link slab (including an enlarged view of the link slab portion) are schematically shown in Fig. 3. Flexural crack formation was expected at the top of the link slab as illustrated in Fig. 3. Therefore, the link slab specimens were designed to include the link slab within the distance between the points of inflection in the adjacent spans. The location of inflection point (depending on the stiffness of the link slab) varies between 0 and 20% of the span length, for the current study - 6.7% was selected. The design procedure for the link slab detail currently requires a debond length of 5% of the simply supported span (Lepech and Li, 2009) and as such, the same debond length was adopted in current study. This debond length requirement was supported by early study (Zia et al. 1995).

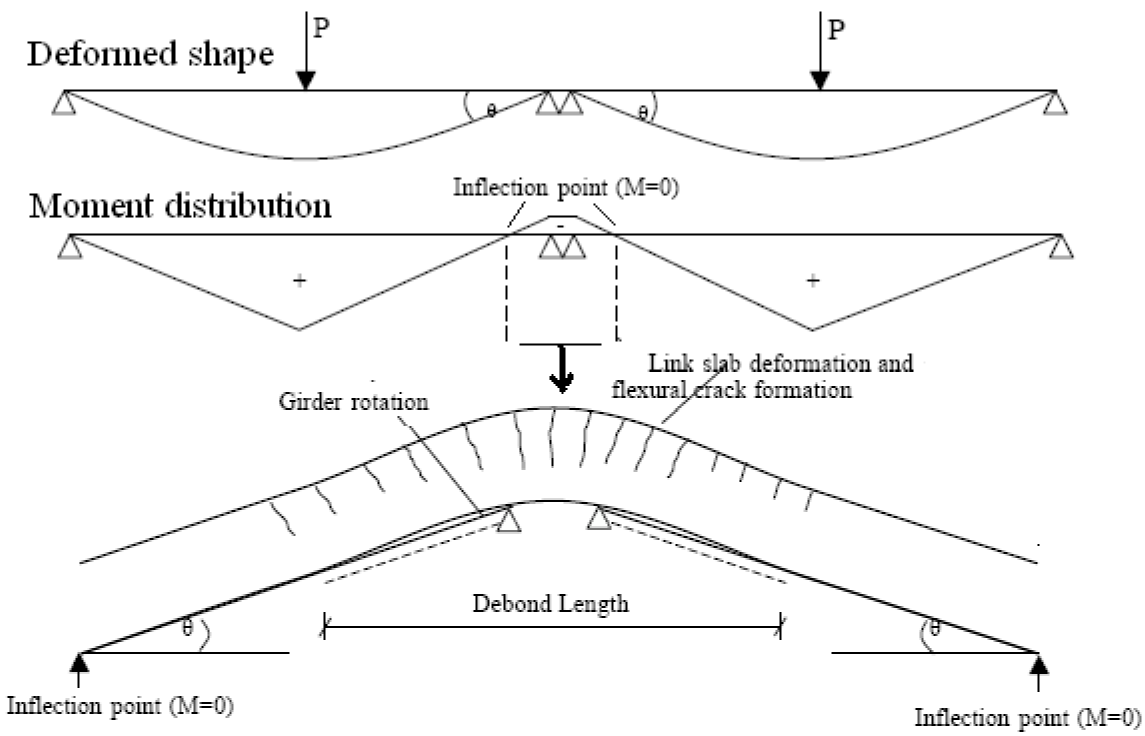

Figure 3: Two span bridge illustrating link slab deformation (between inflection points)

The testing was focused on the link slab portion between the points of inflection in the adjacent spans as illustrated in Fig. 3. Model link slab specimens of 1/4th scale were tested. The dimensions of the representative full-scale bridge deck were 711 mm (width) and 230 mm (depth). Based on this, a typical ¼ scale link slab model had a total length of 930 mm, width of 175 mm and depth of 60 mm. Fig. 4 shows the SCC/ECC link slab specimen geometry showing debond zone length (330 mm) equal to roughly 2.5% of both adjacent spans. Fig. 4 also shows dimensions and reinforcement details of model specimens. Longitudinal reinforcements in the form of three 6 mm bars (reinforcement ratio of 0.01%) were provided. Transverse reinforcements were provided with 6 mm bars at 210 mm c/c. Eight 10 mm shear studs were installed in two rows at each end of the steel I-beam connecting concrete deck.

Mix design of SCC and ECC mixtures used to make link slab specimens are presented in Table 1. The materials used in the production of ECC mixture were Type 10 Portland cement (ASTM Type I), class-F fly ash (FA) with calcium content 5.57%, silica sand (with an average and maximum grain size of 0.30 and 0.40 mm, respectively), polyvinyl alcohol (PVA) fibers (with a diameter of 39 μm and a length of 8 mm) and a polycarboxylic-ether type high-range water-reducing admixture (HRWRA). SCC was produced from

Type 10 Portland cement (ASTM Type I), type "S" slag cement, coarse aggregate with maximum size of 8 to 10 mm, well graded sand and polycarboxylic - ether type HRWRA. ECC was made of Type GU cement (General use type 10 Ordinary Portland cement), Class F fly ash, Polyvinyl Alcohol (PVA) fiber of 8mm length, HRWRA and silica sand with 110 μm average grain size.

For all link slab specimens, adjacent bridge decks (end parts) were cast with SCC. For control SCC link slab specimens (LS-SCC), link slab portion was cast with SCC. For ECC link slab specimens (LS-ECC), link slab portion was cast ECC. The details of link slab specimens are presented in Table 2.

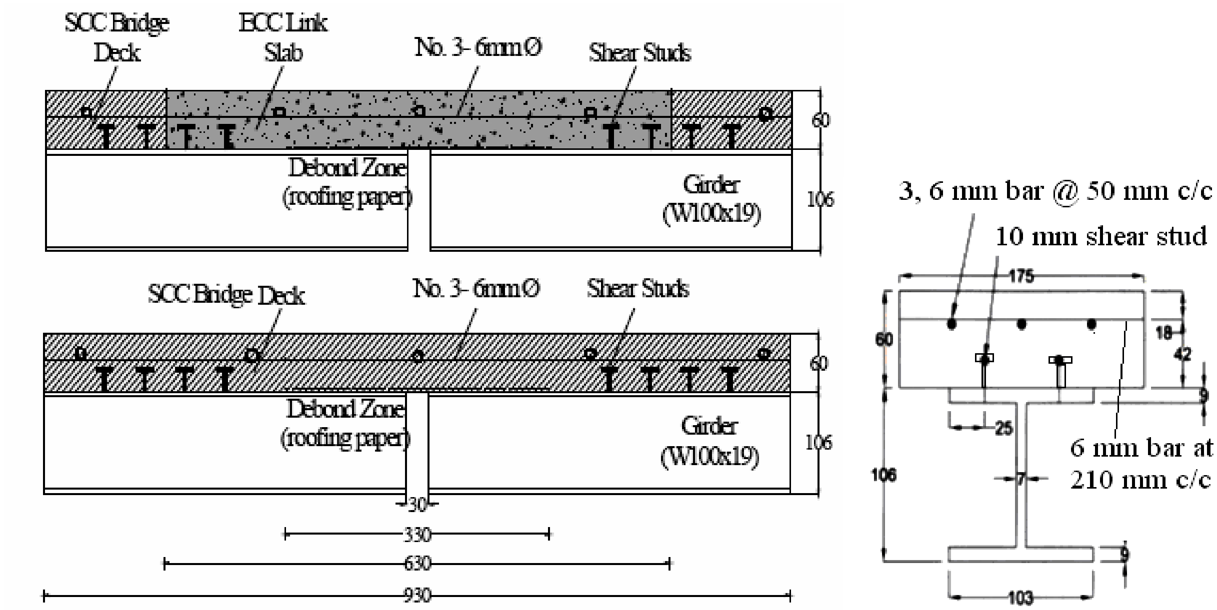

Figure 4: Geometry and reinforcement details of link slab specimens (Dimensions in mm)

Table 1: Mix design of SCC and ECC

SCC ingredients, kg/m^3					
Cement	Slag	Water	Coarse agg	Fine agg.	HRWRA
400	90	172	750	910	1.85
ECC ingredients, kg/m^3					
Cement	Fly ash	Water	PVA fiber	Silica sand	HRWRA
386	847	327	26	448	4.15

Table 2: Dimensions and material composition on different parts of link slab (LS)

Designation	Length	Debonding zone	Transition zone	Concrete type	
	mm	Length (2.5%) mm	Length (2.5%)mm	Transition zone	Debonding zone
LS-ECC	930	330	150	SCC	ECC
LS-SCC	930	330	150	SCC	SCC

For all the link slabs, as followed in the general field practice, the bridge deck part was cast initially and left for setting for 24 hours. After 24 hours, the link slab zone was cast with ECC or SCC. Control specimens in the form of cylinders and beams were also cast at the same time. The specimens were cured for 28 days at the laboratory conditions while covered with burlap. The relative humidity (RH) and the temperature of the laboratory were 45 ± 5% and 24 ± 2°C, respectively. Fig. 5 shows link slab specimens during casting and after casting. The mean yield strength, ultimate strength and modulus of elasticity of 6 mm bar are 407 MPa, 550 MPa and 224 GPa, respectively. The mean compressive strength of ECC and SCC are 45 MPa and 58 MPa, respectively while the mean flexural strength of ECC and SCC are 9.6 MPa and 6.6 MPa, respectively at the age of testing.

Figure 5: Link slab specimens during casting process and after casting

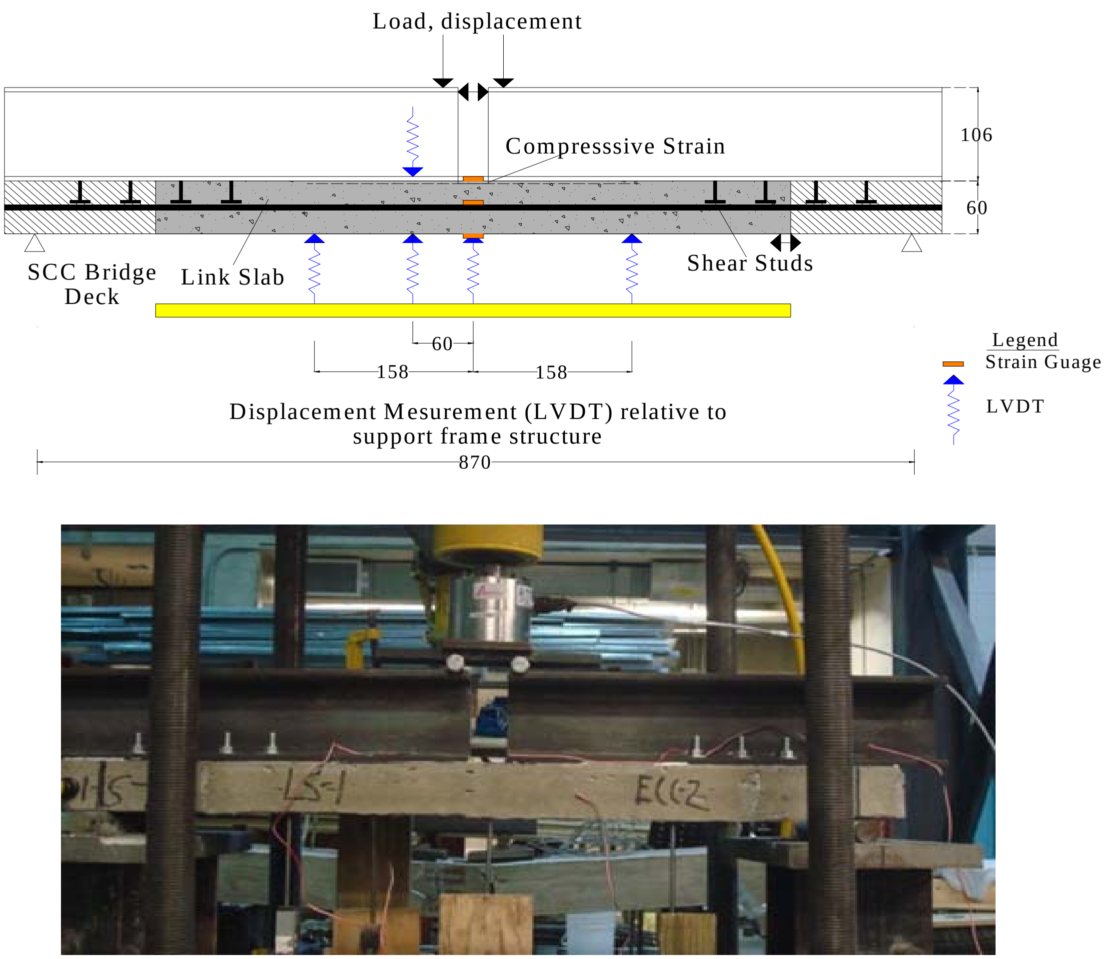

Figure 6: Test-setup, instrumentation and failure modes of specimen (Dimensions in mm)

2.2 Test Set-up, Instrumentation and Testing

The link slab specimens were tested under monotonic loading simulating actual loading and support conditions of the real bridge structure. The test set-up and instrumentation of the link slab showing location of LVDT's and strain gauges are shown in Fig. 6. The test specimen was 930 mm long and supported symmetrically on roller and pin, 870 mm apart. The steel I- girders were separated by a gap of 30 mm at the centre line of the link slab. The stain gauges were installed at the centre of the specimen to monitor the strain development in concrete and reinforcing bars.

The load was applied through a hydraulic actuator at the centre of the test specimen gradually at a rate of 0.05 kN⁄min until failure (Fig. 6). The data was collected with a data acquisition system connected to computer. During testing, the load, displacements and strains in concrete and reinforcing steel of the specimens were monitored. The cracking, crack propagation and failure modes were also visually observed; simultaneously number of cracks and crack width were also noted with the help of crackscope.

3 Results and Discussions

3.1 Load-deflection Response, Crack Development and Failure Modes

For SCC link slab (LS- SCC), a small transverse crack was formed near the mid-span of the link slab at the initial loading phase. The mid-span deflection increased with the increase of load. The crack at the centre gradually grew wider and propagated across the depth to the top of the slab during subsequent loading and led to the failure (Fig. 7).

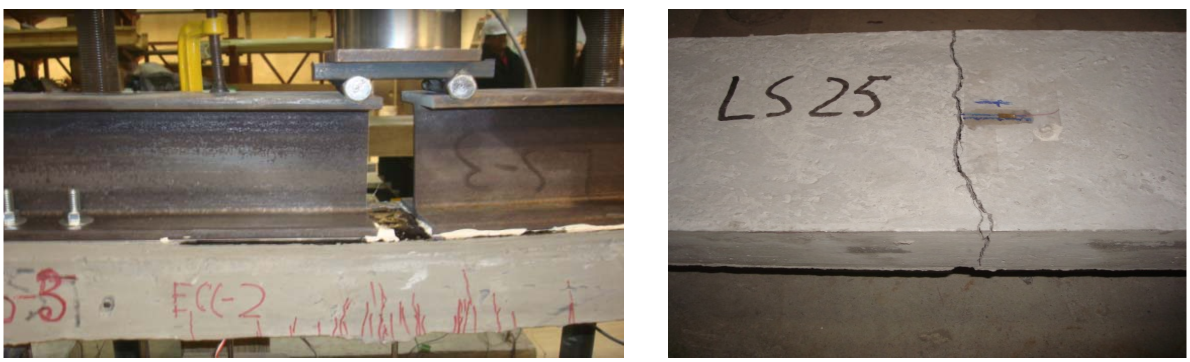

Micro-cracks in LS-ECC — Single crack in LS-SCC

Figure 7: Crack propagation and failure of link slab specimens

In contrast, micro-cracks appeared in at the centre of the ECC link slabs (LS-ECC) in the initial loading stages. With the increase of load, additional hairline micro-cracks formed and propagated across the length of the link slab (Fig. 7). All the crack widths remained below 50 µm and the localization of the crack near the mid-span resulted in the failure of the link slab. Just before the failure of the specimen, the ductile behavior of ECC link slab was visually observed from the deflected shape. On the other hand, SCC link slab showed failure with the formation and propagation of mainly one big crack at the centre. It was also observed that no hairline or micro-crack was formed in the region of transition zone at each side of ECC link slab.

For all the specimens including both SCC and ECC, the cracks generally extended across the entire slab width indicating that the link slab behaved as a flexural member. All the cracks were observed in the debonding zone only and no crack was extended into the deck slab or in the transition zone. This provided with the evidence that the 5% debonding zone was sufficient to keep the stress concentration in the link slab only.

Fig. 8 compares the load-midspan deflection responses of SCC and ECC link slab specimens. Significant differences in the responses were observed. For ECC link slabs, the load-deflection response clearly showed ductile behaviour with strain hardening as evident from the steady increase in deformation with the increase in load. The link slab with SCC failed to show similar strain hardening behaviour. During the loading history, a sudden drop of load was observed at the first peak followed by the formation of a major crack at the centre in the debonding zone (Fig. 8). The load then increased until a second peak was reached with additional deflection. This post-first peak response with large crack width may be associated with the transfer of load to the steel reinforcement (bridging the crack) through steel-SCC bond mechanism. The post first peak response in SCC link slab associated with single crack formation and large crack width is not acceptable for the link slab application.

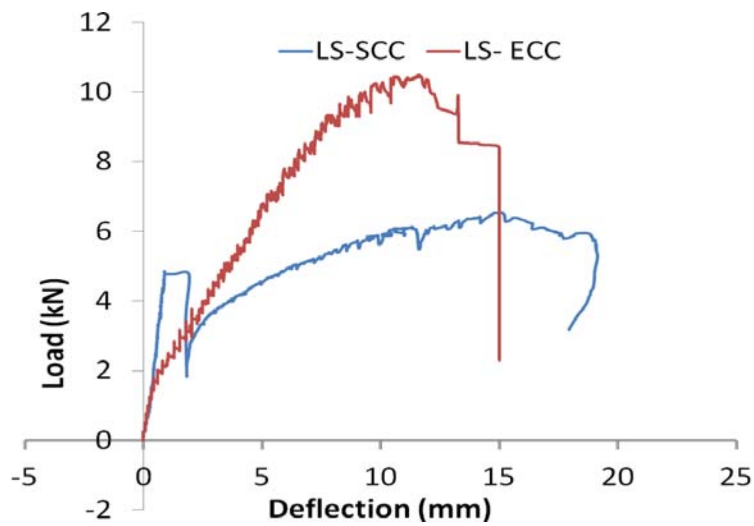

Figure 8: Comparison of load-deflection response

3.2 Strength, Strain Hardening and Energy Absorbing Capacity

Table 3 summarizes the data depicted from load deformation response. The ultimate load of ECC link slab (10.5 kN is much higher than that of SCC (first peak of 4.8 kN and 2nd peak 6.54 kN). Based on the first peak, SCC link slab shows significantly lower load and deflection than its SCC counterpart. Based on first peak, the ductility (strain hardening capacity) of the ECC links slab is significantly higher as evident from the large deflection of 10.5 mm compared to only 1.93 mm of SCC. The energy absorbing capacity of ECC link slab (calculated by the area under the load-deflection curve) was 113 joules compared to 70 joules of its SCC counterpart. While in terms of cracking, ECC link slab developed 48 micro-cracks compared to one major crack in SCC link slab.

Table 3: Strength, strain hardening/ductility and energy absorbing characteristics

	Load (first cracking)	Deflection (first cracking)	Ultimate load	Ultimate Deflection	Number of crack	Energy absorption
	kN	mm	kN	mm		Joule
LS-ECC	3.25	1.50	10.51*	12.22*	48	113
LS-SCC	4.66	1.93	4.8* (6.54)**	0.8* (15.0)**	1 major crack	70

*First peak ** 2nd peak

3.3 Strain Development in Steel and Concrete

Load-steel strain response of the SCC link slab in Fig. 9 shows sudden transfer of load to steel reinforcement at the onset major crack development at the centre (at first peak) and subsequent large strain (stress) development in steel compared to those in ECC link slab. Such stress concentrations in the reinforcement are nonexistent even as the ECC was experiencing micro-crack damage. Subsequently, the yielding of the rebar was delayed in the ECC matrix compared with that in the SCC matrix which is evident from the strain development in rebars (Fig. 9).

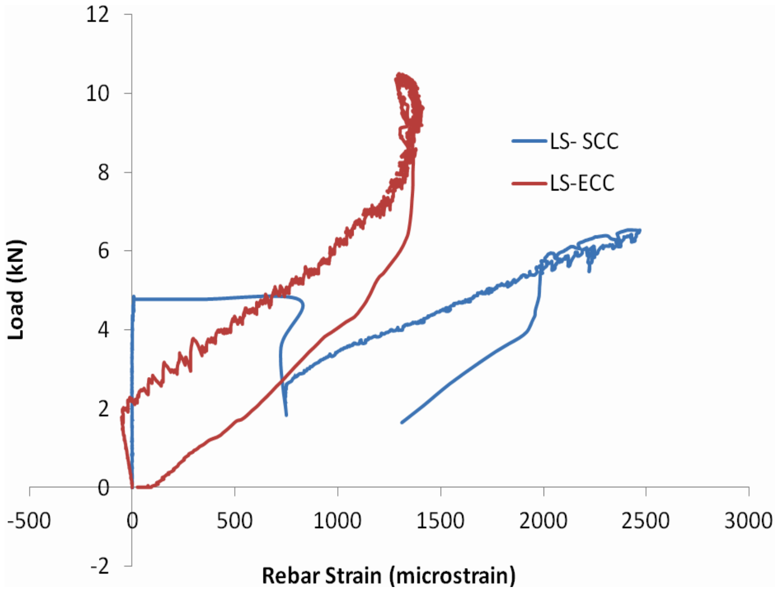

Figure 9: Load-steel strain development in link-slabs

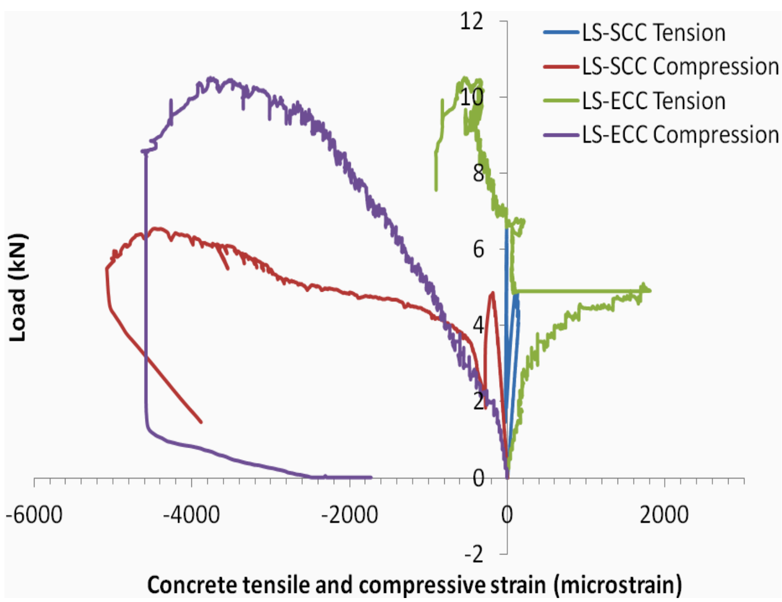

Figure 10: Load-concrete strain development in link-slabs

Steel reinforcement in ECC link slab (strain in steel was around 1300 micro-strain) did not yield even at the ultimate load while yielding of reinforcement was observed in SCC link slab (strain in steel was around 2425 microstrain > yield strain of 2020 micro-strain).

The superior strain hardening capacity of ECC link slab can be attributed to the absence of shear lag between reinforcing bars and the surrounding ECC while the fracture of SCC causes unloading of concrete and transfer of load to the reinforcement resulting in high interfacial shear/bond forces causing failure (Li et al. 2002). Fig. 10 compares the load-concrete strain response of SCC link slab with its ECC counterpart. ECC link slab underwent large tensile strain (1600 micro-strain) compared to its SCC (127 micro-strain) counterpart.

4. Conclusions

This paper compares the structural performance of link slabs (for joint less bridge decks) made with engineered cementitious composite (ECC) and conventional self-consolidating concrete (SCC). Test were conducted on small-scale link slab model specimens of 1/4th scale. The following conclusions are drawn from the study:

- ECC link slab exhibited superior strain hardening behavior over SCC link slab. The inferior strain hardening capacity of SCC link slab can be attributed to the brittle fracture of SCC causing high interfacial shear and subsequent steel-concrete interfacial bond forces. This resulted in higher strain in the rebars in SCC link slab (causing failure due to yielding). On the other hand, formation of micro-cracks in ECC due to bridging action of fibers reduces rebar strain leading to stable strain hardening behaviour suitable for link slab applications.
- ECC link slab showed better performance in terms of higher ultimate strength, higher ductility, better energy absorption capacity, large number of micro-crack formation and small crack width development compared with its SCC counterpart.

The study confirmed the viability of constructing ECC link slabs in joint-free bridge decks with enhanced structural performance.

Acknowledgements

The authors gratefully acknowledge the financial support of Ministry of Transportation of Ontario (MTO) under the Highway Infrastructure Innovations Funding Program. Special thanks to Hannah Schell, David Rhead and Clifford Lam of MTO for their support and assistance.

References

Alampalli, S., and Yannotti, A. P. (1998), In-Service Performance of Integral Bridges and Joint less Decks, *Transportation Research Record* 1624, Paper No. 98-0540, 1-7.

Caner, A. and Zia, P. (1998), Behavior and Design of Link Slabs for Joint less Bridge Decks, *PCI Journal*, 43, 68–80.

Hossain, K.M.A., Maulin, B.M. and Anwar, M.S. (2012), Properties and Structural Performance of Engineered Cementitious Composites with Special Reference to Bridge Applications, Research Report No. STR-01, Department of Civil Engineering, Ryerson University, Toronto, Canada, 45p.

Fischer, G., and Li, V.C. (2003), Intrinsic Response Control of Moment Resisting Frames Utilizing Advanced Composite Materials and Structural Elements, *ACI Structural Journal* 100(1), 166-176.

Fischer, G. and Li, V. C. (2003), Design of Engineered Cementitious Composites (ECC) for processing and workability requirement, vol. 7, *BMC*, Poland, 29–36.

Gilani, A. (2001), Link Slabs for Simply Supported Bridges, incorporating engineered cementitious composites, MDOT SPR-54181. *Structural Research Unit, MDOT*, USA.

Keoleian, G., Kendall, A., Chandler, R., Helfand, G., Lepech, M. and Li, V.C. (2005), Life Cycle Model for Evaluating the Sustainability of Bridge Decks, *Proc. 4th International Workshop on Life-Cycle Cost Analysis and Design of Civil Infrastructure Systems*, Florida, May 8-11.

Lepech, M. D. and Li, V. C, (2009), Application of ECC For Bridge Deck Link Slabs. *RILEM Journal of Materials and Structures,* 42(9),1185-1195.

Li, V.C. (1993), From Micromechanics to Structural Engineering –the Design of Cementitious Composites for Civil Engineering Applications. *ASCE Journal of Structural Mechanics and Earthquake Engineering* 10(2), 37-48.

Li, V.C. (1998), Engineered Cementitious Composites - tailored composites through micromechanical modeling. In: Banthia N, Bentur AA, Mufti A, editors. Fiber reinforced concrete: present and the future. Montreal: *Canadian Society for Civil Engineering,* 64-97.

Li., V. C., Wang, S., Ogawa, A. and Saito, T. (2002), Interface Tailoring for Strain- Hardening PVA-ECC, *ACI Materials Journal*, 99(5), 463–472.

Li, V.C. (2003), Engineered Cementitious Composites (ECC) - A Review of the Material and Its Applications, *Journal of Advanced Concrete Technology*, 1(3), 215–230.

Li, V.C. and Kanda, T. (1998), Engineered Cementitious Composites for Structural Applications, *ASCE J. Materials in Civil Engineering*, 10(2), 66-69.

Sahmaran, M., Lachemi, M., Hossain, K.M.A., Ranade, R. and Li, V.C. (2010), Internal Curing of ECCs for Prevention of Early Age Autogenous Shrinkage Cracking, *Cement Concrete Research*, 39(10), 893-901.

Wolde-Tinsae, A. M., and Klinger, J. E. (1987), Integral Bridge Design and Construction, Report FHWA/MD-87/04, *Maryland Department of Transportation*, USA.

Zia, P., Caner, A. and El-Safte, A. (1995), Jointless Bridge Becks Research Project 23241-94-4, *Center for Transportation Engineering Studies, North Carolina State,* pp. 1-117.